



Hydrophobic hybrid silica sol-gel coating on aluminium: Stability evaluation during saturated vapour condensation

Maria Basso, Elena Colusso, Marco Tancon, Stefano Bortolin, Matteo Mirafiori, Massimo Guglielmi, Davide Del Col, Alessandro Martucci*

Università di Padova, Dipartimento di Ingegneria Industriale and INSTM, Padova, Italy

ARTICLE INFO

Keywords:

Hybrid silica
Sol-gel
Hydrophobicity
Vapour condensation
Durability
Degradation test

ABSTRACT

Hydrophobic coatings are widely employed in liquid-vapour phase change applications, offering advantageous control on condensation dynamics. However, they suffer from poor stability under harsh conditions and their durability is often neglected over thermal performance. Here, the global performance of a hybrid octyl-modified silica coating on aluminium was studied during saturated vapour condensation, in terms of thermal efficiency and durability. The coating successfully promoted dropwise condensation with heat transfer coefficients of $\sim 90 \text{ kW m}^{-2} \text{ K}^{-1}$, an average 9-fold increase with respect to filmwise condensation under similar heat flux conditions. Straightforward and reproducible tests were employed to separately evaluate the different factors influencing the coating's degradation, attempting to reproduce the conditions present in the apparatus used for the condensation experiments. The developed tests could successfully provide a rapid estimation of the coating's durability during a broad range of liquid-vapour phase change applications.

1. Introduction

The efficiency of liquid-vapour phase change (LVPC) has a major influence on both industrial productivity and environmental pollution. Among the LVPC systems, extensive research has been devoted to vapour condensation, which is involved in processes such as water harvesting and heat exchange [1–3]. High efficiency of the latter can be reached by controlling the condensation dynamics. Generally, water vapour condenses on a colder surface either in form of single droplets (dropwise condensation, DWC) or as a uniform liquid film (filmwise condensation, FWC). The presence of a continuous liquid film is known to decrease the heat exchange efficiency, whereas a DWC strongly favours it through a rapid removal of droplets from the condensing surface [4]. During DWC of steam on flat surfaces, the heat transfer coefficient (HTC) can be 5–8 times higher as compared to FWC [5,6].

The LVPC processes are usually related to metallic substrates, which typical hydrophilicity is unfavourable when heat exchange efficiency is considered [4]. However, the condensation mode can be controlled through the surface modification of both chemical composition and morphology. The combination of these two factors allows a fine tuning

of the surface wettability from superhydrophilicity to superhydrophobicity [2,7]. The contact angle hysteresis (defined as the difference between the advancing and receding contact angle) can be reduced by coating the substrate with a lower surface energy material, without nanostructuring the morphology with time-consuming processes. Among the different techniques, silica-based sol-gel coatings offer an efficient trade-off between cost, time, and chemical-mechanical resistance, besides the possibility to properly tune the coating's properties. Their wettability can be controlled through a hybrid organic-inorganic composition, introducing organic groups to decrease the hydrophilicity of plain silica coatings. Experimental results recently demonstrated that such coatings represent a valid strategy for the promotion of DWC on aluminium substrates [6].

Here, the efficiency of an octyl-modified silica sol gel coating was studied during saturated vapour condensation. The high length of the precursor's organic chain is known to increase the hydrophobicity along with the decrease of the contact angle hysteresis [8]. Reductions in average droplet dimension and improvements in condensation HTC were expected, since most of the heat exchanged during DWC is associated to small droplets [9].

Abbreviations: LVPC, liquid-vapour phase change; DWC, dropwise condensation; FWC, filmwise condensation; ACA, advancing contact angle; RCA, receding contact angle; HTC, heat transfer coefficient; PB, pool boiling; OTES, octyltriethoxysilane.; VC, vapour condensation.

* Corresponding author.

E-mail address: alex.martucci@unipd.it (A. Martucci).

<https://doi.org/10.1016/j.nocx.2022.100143>

Received 26 July 2022; Received in revised form 8 December 2022; Accepted 14 December 2022

Available online 15 December 2022

2590-1591/© 2022 The Authors. Published by Elsevier B.V. This is an open access article under the CC BY-NC-ND license (<http://creativecommons.org/licenses/by-nc-nd/4.0/>).

Besides the heat exchange, the introduction of long organic chains in silica networks was recently proven to favour the durability of sol-gel coatings in water-based environments [10]. As recently evidenced by Jin et al. [11], a major challenge for future works is the durability of such coatings, since they face severe environmental conditions when employed in real-life applications (i.e. fouling, scratching, corrosion or high thermal stresses). Among the numerous studies on the control of surface wettability for LVPC devices, the majority primarily focus on developing new paths for surface modification, without considering the coatings' stability over time. On the other side, when the durability is studied, the possible negative influence on the heat exchange is often not examined. An increase in coating's thickness could improve its resistance to harsh conditions but could simultaneously lead to a higher thermal barrier [4,11]. The coatings employed in LVPC applications are therefore required to simultaneously satisfy several tasks, which is a demanding challenge since improving one requisite often implicates worsening another one.

Following our previous work [12], we aimed to evaluate the global performance of a hybrid octyl-modified silica coating during saturated vapour condensation. The heat exchanged over time was examined on aluminium substrates in a custom-made heat exchange apparatus. The coating's stability was studied by separating the different influencing factors on its degradation, from temperature to steam-air coexistence to nucleation and growth phenomena. The coating's degradation, which led to variations in thickness, wettability, chemical and morphological properties, was monitored with scanning electron microscopy, Fourier-transformed infrared spectroscopy, ellipsometer and goniometer characterizations.

2. Materials and methods

2.1. Materials

Tetraethylorthosilicate (TEOS, 98%; Sigma Aldrich), octyltriethoxysilane (OTES, 98%; Sigma Aldrich), absolute ethanol (EtOH, Emsure; Sigma-Aldrich), concentrated hydrochloric acid (HCl, 37%; Sigma Aldrich), milliQ water (H₂O, 18.2 MΩ). All employed materials were used as purchased, except for hydrochloric acid which was diluted to obtain a 1 M concentration. Silicon wafers, aluminium with high purity (AW1050, 99.50% minimum aluminium content), 20 × 20 mm² and 20 × 50 mm² dimensions. Aluminium was polished to obtain a smooth mirror-like surface, following a standard metallographic technique.

2.2. Synthesis of precursor solution

The octyltriethoxysilane-based solution was prepared adapting a recipe from De Ferri et al. [8] TEOS, OTES, EtOH, HCl 1 M and H₂O were mixed in molar ratios of (TEOS+OTES):EtOH:H₂O:HCl = 1:2:2:0.01, respectively, with variable TEOS:OTES molar ratio. The solution was stirred for 2 h at 400 rpm at room temperature, during which additional solvent was added after 30 min, to reach a theoretical final concentration of SiO₂ of 1.3 M. The solution was aged still for 2 additional hours and then filtrated with syringe filters of 0.2 μm pores prior to the deposition.

2.3. Deposition of hybrid silica coatings

The sol-gel coatings were deposited on polished aluminium substrates and silicon wafers, both previously cleaned through sonication in ethanol followed by atmospheric plasma treatment (Plasma Cleaner, PDC-002-CE, Harrick Plasma). The deposition was done inside a custom-made dip-coater, by withdrawing the substrates from the solution at 4.8 cm/min. The solvent evaporation was induced gradually, together with the evolution of condensation reactions, by aging the coatings at room temperature for 24 h. The coatings were then annealed in a furnace at 200 °C for 2 h, with a heating ramp of 10 °C/min.

2.4. Saturated vapour condensation experiments

The hybrid silica coatings deposited on aluminium substrates were tested in a two-phase thermosyphon designed for the investigation of water vapour condensation (VC) on vertical metallic substrates. The test rig, the experimental procedure, the data reduction technique, and the uncertainty analysis are fully described in Mirafiori et al. [13] Briefly, the experimental apparatus consists of three main components: a boiling chamber, a test section, and a post-condenser (Fig. S1). The design of the test section allows to simultaneously measure the heat transfer and visualize the condensation phenomenon. The vapour produced inside the boiling chamber flows into the test section where it is partially condensed over a metallic sample (condensing area: 50 mm high, 20 mm wide). Inside this component, condensation is driven by the action of the cooling water supplied on the back surface of the sample by a thermostat bath at controlled temperature and flowrate. Downstream the test section, the two-phase mixture (vapour and liquid) is completely condensed in the post-condenser before returning to the boiling chamber. The video acquisition system consists of a powerful LED and a high-speed camera Photron FASTCAM UX100 coupled with a macrolens. Details about the calculation of the heat transfer coefficient are reported in the Supporting Information. Condensation tests to assess the coating robustness over time were performed at the following thermodynamic conditions: 106 °C of saturation temperature (which corresponds to a saturation pressure of 1.24 bar), 2.9 m s⁻¹ of steam velocity, heat flux in the range 250–550 kW m⁻².

2.5. Degradation tests

The coatings deposited on silicon substrates were tested under five different environments that could affect the coating's degradation and could be related to the conditions present during the condensation experiments. The tests were chosen to be straightforward to perform and easily replicable. The exposure time of each tested condition was set to 7 h, to be comparable to the condensation experiments. Three main factors were considered separately and then combined: the chemical-mechanical interaction with water, the effect of temperature and the role of defects. The effect of the hot water on the coatings was considered both in the case of liquid and vapour phase (i.e., steam-air mixture). The five different tests are summarised in Fig. 1. A first sample was heat treated at 100 °C in a standard heating furnace (T-100). A second specimen was exposed to an air-steam mixture, during which the coated surface was held downside in a horizontal position, 3 cm above a glass beaker containing boiling deionized water (S-100). The third and fourth samples were fully immersed in a glass beaker containing deionized water at 20 °C (I-20) and 90 °C (I-90), respectively, whereas the last sample was immersed in boiling water (pool boiling, PB). To further correlate the influence of the substrate type on the coating's stability, the PB test was carried on a reference coated aluminium sample as well (PB-Al).

2.6. Characterizations

A J.A. Woollam Co. spectroscopic ellipsometry (Woollam M2000) was used to measure the thickness of plain coatings at incident angles of 65°-70°-75°, in a 300–1200 nm range. The experimental data were fitted with Cauchy models and the final value was obtained by averaging three distinct points on the same sample. Fourier-transform infrared (FTIR) spectroscopy measurements were conducted with a Jasco FT-IR 4200 spectrophotometer equipped with an ATR ProOne attachment. Measurements on coatings deposited on silicon substrates were collected in transmission in the 4500–400 cm⁻¹ range, at 64 scans min⁻¹ and with a resolution of 2 cm⁻¹, by doing the background with a monocrystalline silicon wafer. Samples on aluminium substrates were analysed in attenuated total reflectance (ATR) mode, by setting the same parameters used for the silicon samples and collecting a background in air. The

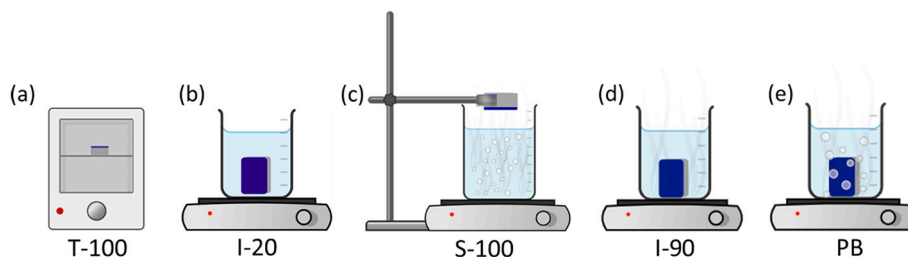


Fig. 1. Different conditions used in the degradation tests on silicon substrates: (a) heat treatment at 100 °C in furnace (T-100); (b) immersion in deionized water at 20 °C (I-20); exposure to mixed air-steam (S-100); (d) immersion in deionized water at 90 °C (I-90); (e) immersion in boiling water at 100 °C (PB). Scheme drawn using <http://Chemix.org> editor [14].

surface morphology was investigated with a field emission scanning electron microscope (FE-SEM, Zeiss Sigma HD) with a secondary electron detector, operating at 5KV. The dynamic contact angles (advancing – ACA, and receding – RCA) were measured with an addition-removal method, by dispersing and subsequently withdrawing a water droplet of approximately 5 μL volume. The measurements were conducted with the aid of a home-made set-up consisted of a DCC1545M CMOS sensor camera (Thorlabs GmbH®, Bergkirchen, Germany) and MVL7000 sensor lens (Thorlabs GmbH®, Bergkirchen, Germany).

3. Results

3.1. Optimization of hybrid-silica coating

We first considered the effect of the OTES/TEOS ratio and the deposition parameters on wettability, thickness, and adherence to the substrate. Preliminary experiments were performed on silicon by tuning the moles of OTES from a minimum of 10% (O1T9) to a maximum of 50% (O5T5) to TEOS, testing different withdraw speeds (from 2.5 cm/min up to 10 cm/min). Dewetting of the coatings were observed for O4T6 and O5T5. Therefore, these compositions were discarded.

As reported in Table 1, the amount of OTES affected the surface wettability by increasing the ACA from $100 \pm 2^\circ$ to $106^\circ \pm 2^\circ$ and the RCA from $88 \pm 1^\circ$ to $96 \pm 2^\circ$. Based on previous results of other hybrid silica-based systems [15,16], we expected an enhancement of the HTC during dropwise condensation due to the higher ACA and low hysteresis of the OTES/TEOS coatings. The hysteresis for all the compositions is in the range of $10\text{--}14^\circ$, slightly lower than other hybrid organic-inorganic coatings obtained by different molecular precursors (e.g. phenyltriethoxysilane and methyltriethoxysilane) [12].

The thickness of the films, evaluated by ellipsometry, was between 200 and 400 nm. These values can be considered a good compromise to ensure adequate robustness in harsh environment (high temperature and heat flux) and minimize the thermal resistance of the deposited

Table 1

Thickness, advancing contact angle (ACA) and receding contact angle (RCA) of the coatings on silicon for different OTES/TEOS molar ratio and withdrawal speed.

Sample	Withdrawal speed (cm/min)	Thickness (nm)	ACA ($^\circ$)	RCA ($^\circ$)
O1T9–5 cm/min	4.8	216 ± 2	100 ± 2	88 ± 1
O1T9–7.5 cm/min	7.4	248 ± 8	101 ± 1	89 ± 1
O2T8–5 cm/min	4.8	227 ± 5	101 ± 1	88 ± 1
O2T8–10 cm/min	10.4	330 ± 7	103 ± 1	91 ± 1
O3T7–2.5 cm/min	2.5	207 ± 6	105 ± 1	96 ± 1
O3T7–5 cm/min	4.8	343 ± 9	106 ± 2	96 ± 2

coating, which affects the overall condensation performance. Hybrid silica-coatings with thickness < 200 nm have been proven to degrade in the first 15 h of condensation [16]. Considering a film thickness between 200 and 400 nm and a thermal conductivity of $0.2 \text{ W m}^{-1} \text{ K}^{-1}$, the thermal resistance per unit area of the developed coatings can be estimated in the range $1.5\text{--}2 \text{ m}^2 \text{ K MW}^{-1}$ [12].

Further samples were deposited on polished aluminium substrates ($2 \times 2 \text{ cm}^2$), selecting O2T8 and O3T7 compositions at a fixed withdrawal speed of 4.8 cm/min. As previously observed [17], the change of substrate causes a slight increase in thickness, attested to about 300 nm for O2T8 and 380 nm for O3T7. The wettability was similar for both the compositions, with average ACA of $102 \pm 3^\circ$, and RCA of $89 \pm 3^\circ$. In light of these results, we selected the O2T8 composition as a good compromise in terms of wettability, thickness and reproducibility. Following the same protocol, the O2T8 coating was deposited on a larger aluminium substrate ($5 \times 2 \text{ cm}$) for vapour condensation (VC-Al) tests.

3.2. Condensation experiments

The heat transfer performance of the hybrid silica sol-gel coating, selected to be O2T8 from the previous section, was assessed during steam condensation in the custom-built experimental apparatus, as described in Section 2. During the test runs, the heat flux was varied between 250 kW m^{-2} and 550 kW m^{-2} , while saturation temperature and steam velocity were kept constant at 106°C and 2.9 m s^{-1} , respectively. The experimental results of the VC-Al test are shown in Fig. 2 (a), in which the HTC is plotted versus time.

The functionalized surface sustained DWC for the entire duration of the condensation tests (i.e., 7 h), exhibiting a stable thermal performance with HTC values of $\sim 90 \text{ kW m}^{-2} \text{ K}^{-1}$. No changes of the coated surface were detected from the thermal measurements since the HTC remained almost constant for the whole endurance tests. During the test runs, the heat flux was reduced from 550 to 250 kW m^{-2} to assess the effect of the heat flux on HTC (Fig. 2 (a)). Due to the fixed value of the saturation temperature, the temperature of the cooling water supplied to the test section was varied between 25°C and 85°C to control the heat flux. The latter increases with the increasing saturation-to-coolant temperature difference. In accordance with literature [18,19], the HTC measured during DWC was found to be constant in the heat flux range here investigated ($250\text{--}550 \text{ kW m}^{-2}$), despite the considerable variation of coolant temperature. Interestingly, similar heat flux values could be obtained during FWC only with the HTC being significantly lower ($8\text{--}12 \text{ kW m}^{-2} \text{ K}^{-1}$ according to the FWC model described in Del Col et al. [20]). Therefore, in the present work, the promotion of DWC on aluminium substrates resulted in an average 9-fold increase of the condensation HTC compared to values measured during FWC under similar heat flux conditions [20]. If compared to other sol-gel coatings with slightly higher wettability (average ACA of about 90°) and similar film thickness, which were tested during DWC under the same heat flux condition, the developed coating showed an increase in the HTC of about 10% [12].

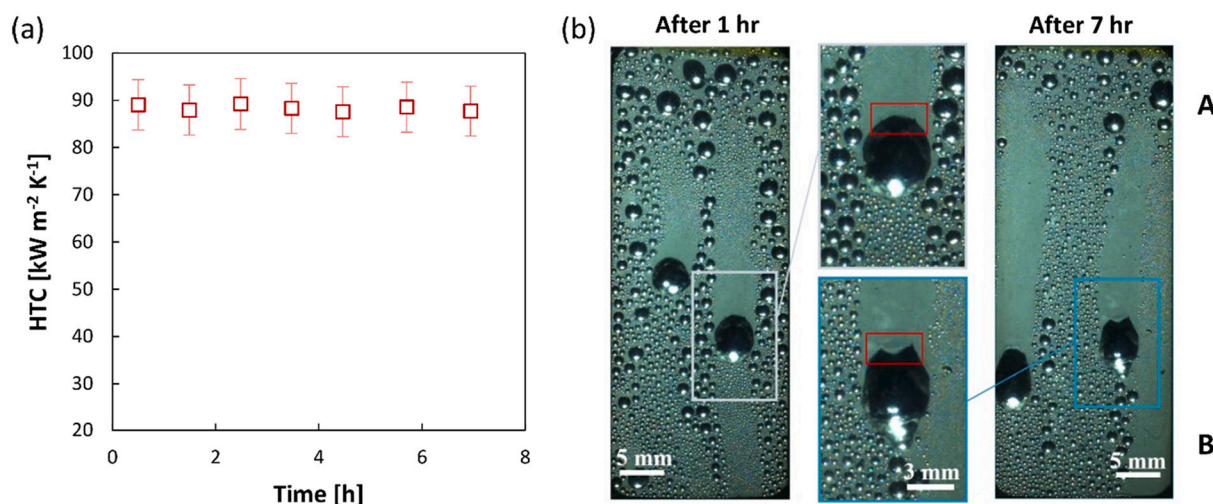


Fig. 2. (a) Heat transfer coefficient (HTC) measurements obtained during DWC of steam on the sol-gel coated aluminium sample versus time. (b) Images recorded at the beginning and at the end of the condensation test. An example of droplet pinning is shown. The position of the two examined areas of the coated surface (top and bottom) is highlighted by the letters A and B, respectively.

The images taken at the beginning and end of VC-AI tests showed an evolution of the condensation phenomenon, specifically of the droplet population (Fig. 2 (b)). The droplet's departing radius, which is a key parameter of the DWC heat transfer mechanism, showed a moderate increase after 7 h in some areas of the sample, from 1.1 mm to 1.5 mm. Being the thermodynamic conditions constant [21], the droplet's

departing radius depended on the surface wettability, therefore a variation of the contact angles was expected. This variation could also be related to an increase of the droplets' pinning, which affects their motion on the condensing surface (Fig. 2 (b), zoomed images). Even though no variations in the HTC were detected after 7 h of continuous condensation, the experiments were stopped to investigate the evolution

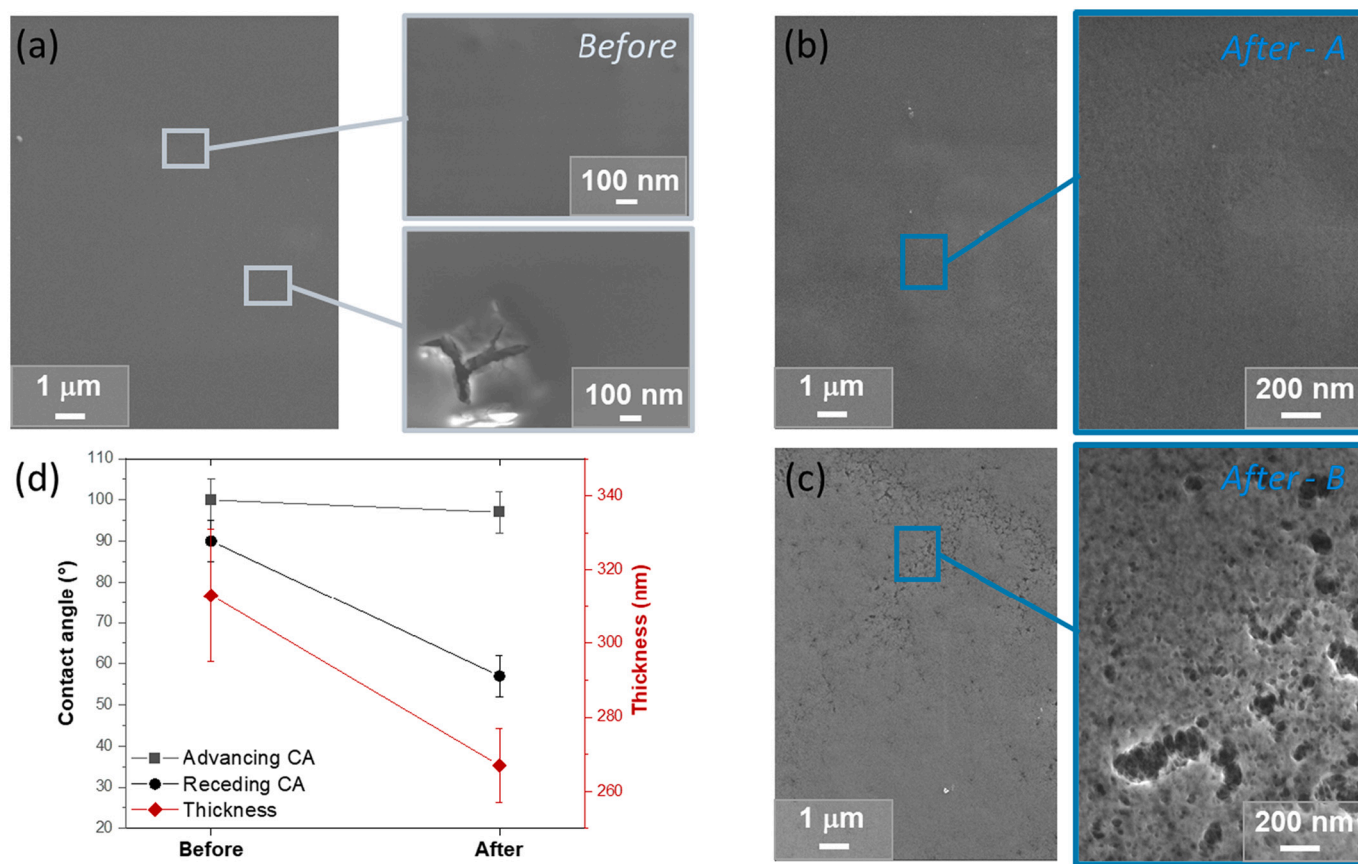


Fig. 3. (a-c) SEM images of the octyltriethoxysilane-based coating on aluminium: (a) reference sample; (b) sample after the 7 h condensation tests (VC-AI), on zone A; (c) sample after the 7 h condensation tests, on zone B. The scale bar of each figure is reported on the bottom right. (d) Variation of the dynamic contact angles and of the coating's thickness after the 7 h VC-AI tests. Each experimental result is the average value of three distinct measurements in different areas of the sample. The standard deviation is reported for each result.

of the coated surface before that irreversible and complete degradation could be reached.

The changes in the dynamic contact angles, thickness, and morphology of the coatings after 7 h of continuous condensation are reported in Fig. 3, while the FTIR spectroscopy results are visible in Fig. S2. Before the VC-Al tests, the coated aluminium surface was hydrophobic, with advancing contact angle (ACA) of $100 \pm 5^\circ$ and receding angle (RCA) of $90 \pm 5^\circ$. The ellipsometry measurements revealed an initial coating thickness of 310 ± 18 nm. After the condensation tests, the thickness moderately decreased by ~ 46 nm, along with a decrease of $\sim 33^\circ$ of the RCA. According to FTIR spectroscopy, no variations in the vibrational modes of the peaks could be observed. The vibrational peak at ~ 1180 cm^{-1} , corresponding to the bond between octyl-groups and silicon ($\text{Si-CH}_2\text{-(CH}_2\text{)}_6\text{-CH}_3$), was covered by the intensity of Si-O-Si bonds, therefore it could not be used to evaluate the possible disappearance of the organic groups [8]. Nonetheless, the persistence of a hydrophobic character was shown by the ACA, which was not affected after 7 h of condensation ($\text{ACA} = 97 \pm 5^\circ$, Fig. 3 (d)). FTIR spectroscopy is commonly used to monitor the evolution of hydrolysis and condensation reactions, via the ratio between the peak of asymmetric stretching of Si-O-Si (~ 1120 cm^{-1}) and Si-OH peak (~ 940 cm^{-1}) [22]. We did not see any evident network variations, since the ratio between the Si-O-Si and Si-OH peaks did not vary after the condensation experiments (Table S1).

Significant variations in the coating's morphology after the exposure to saturated vapour were instead highlighted by SEM (Fig. 3 (a-c)). During the VC-Al tests, droplet pinning was not observed as a global and homogeneous phenomenon but was instead present only at isolated locations. In the afterwards characterisations, several macro-areas were explored to detect possible morphological variations and wettability differences. Two different representative areas were individuated, namely at the top (zone A - Fig. 3 (b)) and at the bottom (zone B - Fig. 3 (c)) of the sample, and their position is reported in Fig. 2 (b). As shown in the insights at higher magnification (Fig. 3 (a-c)), the interaction with saturated vapour during condensation led to an evolution of the coating. Prior to the tests, the sample's surface was globally smooth and uniform, presenting only a few isolated and small defects such as nanocracks (Fig. 3 (a)). After the 7 h condensation tests, local spots of the surface were found to gradually evolve into a spiderweb-like morphology characterized by a higher porosity (Fig. 3 (a-c)). Similar morphologies were found by Metroke and coworkers, which studied the corrosion resistance in salt-containing environments [10]. Here, the spiderweb morphology of the coating was found to be more pronounced on the bottom (Fig. 3 (c)) with respect to the top part (Fig. 3 (b)) of the sample. The RCA on zone B ($63 \pm 5^\circ$) was slightly lower respect to zone A ($70 \pm$

5°), and ellipsometry detected a thickness decrease in the bottom area of ~ 60 nm, slightly higher respect to the average value (~ 46 nm).

3.3. Degradation tests

From the characterizations carried out before and after condensation experiments (Section 3.1), the evolution of the hybrid silica sol-gel coating seemed to be related to the combined effect of mechanical-chemical interaction with water, high temperature of the environment, and presence of defects/voids on the coating. To investigate the effect of steam condensation on the coating's stability, ad-hoc tests were performed as described in Sec. 2 to separate the different variables of influence.

The evolution of advancing and receding contact angles is reported in Fig. 4 (a, b). Coherently for both angles, the wettability was affected the most by the pool boiling test (PB), in which vapour bubbles nucleated on the coated surface. The ACA decreased by $\sim 30^\circ$ and by $\sim 10^\circ$ after pool boiling and immersion at 90°C , respectively, whereas the other tests did not lead to significant variations. Analogously, the RCA showed a similar trend, but with enhanced variations. After PB test, the RCA decreased below the measurable limit, while I-90 and I-20 tests led to reductions of $\sim 41^\circ$ and $\sim 13^\circ$, respectively. The exposure to hot steam-air mixture (S-100) and the heat treatment at 100°C (T-100) did not affect the RCA. The latter result was expected, since the hybrid coatings were exposed to temperatures of 200°C during the annealing treatments (Section 2, deposition paragraph).

As for the aluminium sample, FTIR spectra were collected on the coated silicon samples to detect eventual chemical modifications caused by the degradation tests (Fig. 4 (c)). The ratio between the intensities of the Si-O-Si peak (~ 1078 cm^{-1}) and the silanol peak (~ 950 cm^{-1}) was monitored to detect changes in the network, but no evident variations were noticed (Table S2). The thickness before and after the degradation tests is reported in Table S3. Globally, the tests did not lead to changes in thickness, except for the pool boiling test, after which the coating's thickness decreased by ~ 80 nm.

The morphologies of the coatings after PB and I-90 tests are reported in Fig. 5 (b, c) in comparison to a reference sample (Fig. 5 (a)). As visible from the SEM images, the latter's morphology was found to be smooth, flat, and uniform in the nano and microscale. After the degradation tests, the pool boiling led to the highest deterioration of the coating's quality, with the appearance of surface features on the nanoscale (Fig. 5 (b)). Respect to the I-90 test, the PB test led to nucleation and growth of vapour bubbles on the coated surface, which accelerated the formation of the nanofeatures visible in Fig. 5 (b). The latter were only slightly detectable after the immersion test at 90°C , whereas the S-100, I-20 and

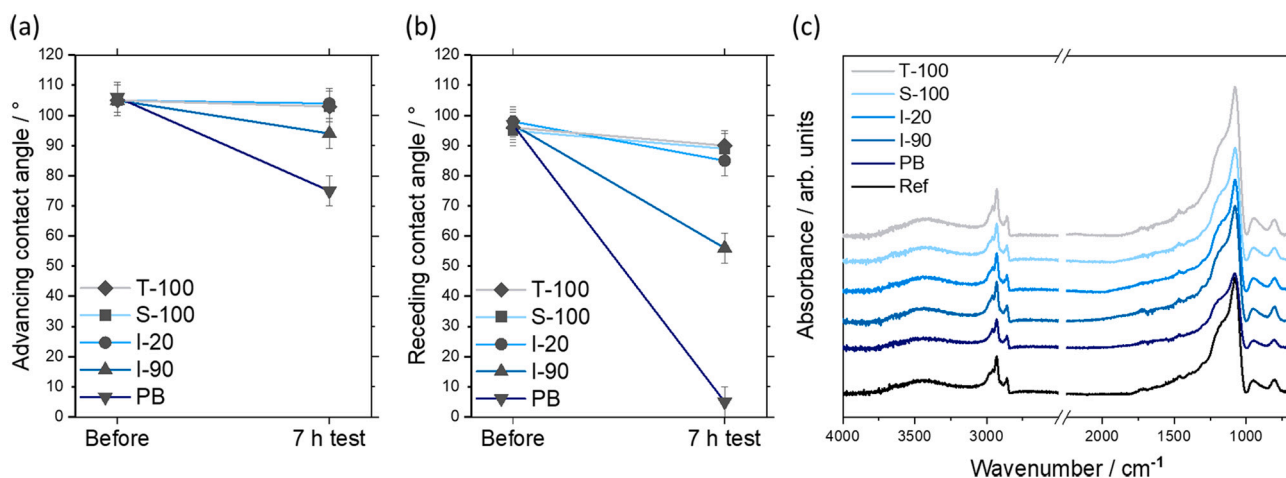


Fig. 4. (a, b) Dynamic water contact angles of the hybrid silica coatings deposited on silicon, before and after the degradation tests: (a) advancing contact angles (ACA); (b) receding contact angles (RCA). (c) FTIR spectroscopy absorption spectra of the reference sample and of the coatings after the degradation tests.

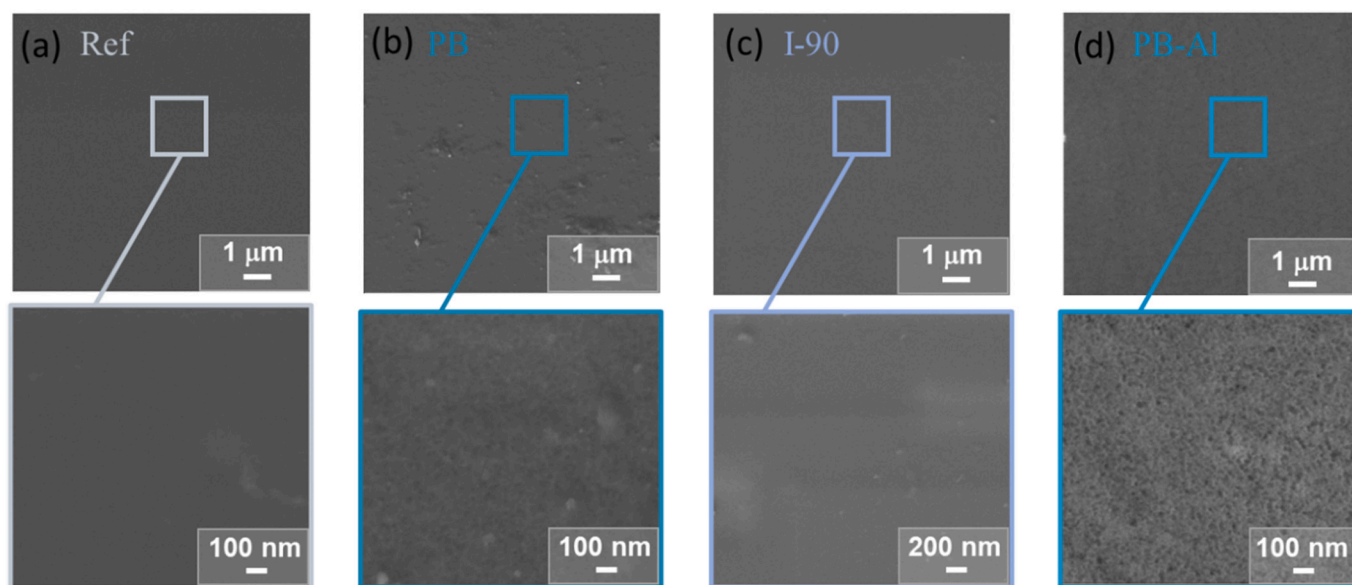


Fig. 5. SEM images of the hybrid silica coating on silicon and aluminium substrates after the 7 h degradation tests, at 2 different magnifications. (a) reference sample on silicon; (b) coating on silicon after pool boiling immersion test (PB); (c) coating on silicon after immersion test at 90 °C (I-90); (d) coating on aluminium after pool boiling immersion test (PB-Al). The scale bar of each figure is reported on the bottom right.

T-100 tests did not induce significant variations of the surface morphology.

To consider the possible influence of the substrate on the coating's degradation, the PB test was repeated on a coated aluminium sample (PB-Al). The variations in contact angles, thickness and morphology are reported in Fig. 5 (d) – S3 and Table S4. In analogy with the PB test on silicon, the RCA decreased below the measurable limit (from $87 \pm 5^\circ$ to $< 10^\circ$), whereas the ACA remained unchanged. As for both PB test on silicon and VC-Al test, the thickness decreased by ~ 40 nm (from 266 ± 10 to 228 ± 7 nm) and the initially smooth surface morphology evolved after the test, after which the formation of nanofeatures was detected (Fig. 5 (d)).

4. Discussion

As discussed in the Introduction section, coatings employed in heat transfer applications are simultaneously required to fulfil two main purposes: the control of condensation dynamics and the durability during their industrial employment. In this work, we initially tested the thermal performances of a hybrid silica sol-gel coating during DWC of steam in a custom-made apparatus (VC-Al test, Fig. S1). The coating, deposited on an aluminium substrate, induced DWC with HTC values of $\sim 90 \text{ kW m}^{-2} \text{ K}^{-1}$, ~ 9 times higher with respect to HTC measured on hydrophilic aluminium at similar heat flux conditions [20].

HTC values above $100 \text{ kW m}^{-2} \text{ K}^{-1}$ and extended durability were reported for copper-modified surfaces [23,24]. Compared to copper, studies about DWC on aluminium are limited. Paxson et al. reported HTC value of $35 \text{ kW m}^{-2} \text{ K}^{-1}$ stable for up to 48 h on aluminium substrates covered with an ultrathin polymer film deposited by iCVD [25]. Raush et al. demonstrated a duration of DWC for 8 months on ion-implanted aluminium, but the HTC was only double compared to FWC [26]. Steam or liquid at high temperature ($> 100^\circ \text{C}$) promotes the formation of boehmite on the aluminium surface, enhancing the wettability and thus affecting the durability of the DWC conditions.

Despite the morphological and functional variations of the hybrid silica sol-gel coating during steam condensation, the HTC remained stable for the entire duration of the condensation experiments without any significant variation of the thermal performance, in accordance with our previous results on similar hybrid coatings [12]. The VC-Al test was stopped after 7 h to properly characterize the coating variation and

avoid its total failure. A decrease in thickness of ~ 46 nm was found, along with morphological and wettability variations. Two different representative areas were individuated on the coating, indicating a non-uniform degree of degradation on its surface (Fig. 3 (b, c)). Since the vapour flow was almost constant along the sample, the different evolution among the two areas could be attributed to the non-uniform interaction with the condensate. Due to the vertical orientation of the sample, the upper area was less affected by the sweeping of falling drops as compared to the lower part. On this lower part, the chemical-mechanical interaction between the coating and the water was higher due to a higher condensate mass flow rate. The presence of small defects such as microcracks or pinholes, which were seen in a few spots on the initial coating (Fig. 3 (a)), contributed to locally accelerate the coating's degradation as found in previous studies [12,27,28]. Droplets' nucleation on pre-existing defects, along with shear stress applied by their sweeping over the defects, can enlarge the dimensions of the latter leading to the gradual delamination of the coating. In the lower area of the sample, the frequency of droplets' nucleation was higher, as well as their sweeping, which could have contributed to the enhanced modifications of the coating's morphology. Moreover, the presence of unreacted hydrophilic silanol groups on the surface can promote the interaction with condensing saturated vapour. Respect to other hybrid sol-gel coatings [11], the low temperature of thermal degradation of octyl-groups does not allow to perform the coating's annealing above 200°C ⁸, leading to the presence of residual hydrophilic Si-OH groups. The durability of surface hydrophobicity is therefore a crucial factor to reduce the affinity and interaction with condensed vapour, as found by Juan-Diaz et al. [29] Breakage of organic-silica bond and/or partial removal of the coating on the underlying substrate could lead to the decrease of contact angles [29,30], since both the factors lead to the exposure of hydrophilic spots among the surrounding hydrophobic area. However, as described in the Results section, no major chemical variations were noticed from FTIR spectroscopy, so the local morphological changes (Fig. 3 (c)) can be the major cause of the RCA decrease.

In the second part of the work, ad-hoc degradation tests were performed to separate the different influencing factors on the coating's durability. Neither the chemical interaction with water (I-20) or air-vapour stream (S-100) nor the exposure to high temperatures (T-100) induced significant variations in the coating's properties (Fig. 4). The tests evidenced how these factors, if applied singularly, were not

sufficient to induce remarkable changes in the coatings. Variations in wettability and morphology were seen when the interaction with water was combined with higher temperatures (I-90), whereas the maximum deterioration was reached when bubble nucleation was induced (PB and PB-Al). The simultaneous presence of all factors led to the highest degradation, as confirmed by the substantial decrease of dynamic contact angles and thickness (Fig. 4, Table S3 - S4). On both silicon (PB) and aluminium (PB-Al) substrates, the formation of features at the nano-microscale led to pinning of water droplets and affected the RCA at the macroscopic scale, leading to its decrease below the measurable level.

Analogously to bubble nucleation during PB and PB-Al tests, during the condensation experiments nucleation, growth and sweeping of condensed vapour droplets were identified as crucial factors for the coating's degradation. After the VC-Al test, the formation of the nano-features was not detected on the whole surface, except for local spots on the lower area, in which a porous spiderweb morphology was found. Globally, the pool boiling test was found to be more aggressive on both silicon (PB) and aluminium (PB-Al) with respect to the VC-Al test, in terms of changes in wettability and overall morphology (Fig. 3 (d) - 4 (a, b)). The PB test was found to induce similar variations in wettability, thickness, and morphology on both the silicon and aluminium substrates (Fig. 4-5, Table S3 - S4), whereas the wettability changes induced by the I-90 test were similar to the ones found after the VC-Al test (Fig. 3 (d) - 4 (a, b)). A non-identical behaviour between PB-Al and VC-Al tests was expected, due to the different nature of the two processes: on the former, the coatings were fully immersed in boiling water and air bubble nucleation was developed, whereas on the latter, the sample was exposed to a saturated vapour flux and water droplets condensed on its surface. However, the changes in thickness and morphology found on the two samples showed interesting similarities (Fig. 3 (b) - 5 (d)).

The stability tests on silicon or metallic substrates can therefore provide a useful tool to induce an accelerated degradation on the coatings, to evaluate their resistance under harsh conditions before their employment on larger scale applications. Based on a reproducible and straightforward approach, the proposed tests allow to separately study the different influencing factors, that can be then partially (I-90) or totally (PB) combined according to specific performance requirements.

5. Conclusions

In this work, the heat transfer performance of a hybrid silica sol-gel coating was tested in a custom-made apparatus during the condensation of saturated vapour. The coating successfully promoted DWC with HTC values of $\sim 90 \text{ kW m}^{-2} \text{ K}^{-1}$, an average 9-fold increase with respect to FWC under similar heat flux conditions [20]. The heat transfer performance remained stable during the overall duration of condensation experiments, which were stopped prior to a possible failure to investigate the detected changes in wettability and morphology. Straightforward accelerated degradation tests were performed to separate the different influencing factors, to evaluate the coating's resistance prior to its real industrial application. If singularly applied, the possible degradation conditions did not lead to significant variations on the coating's properties, whereas the interaction with water at high temperature induced different degrees of degradation whether if bubble nucleation was present (PB) or avoided (I-90). Thanks to similar variations in wettability and morphology, the latter tests could successfully provide an estimation of the coating's durability during a broad range of LVPC applications.

Declaration of Competing Interest

The authors declare that they have no known competing financial interests or personal relationships that could have appeared to influence the work reported in this paper.

Data availability

Data will be made available on request.

Acknowledgments

E.C. and A.M. acknowledge funding through the SID project BIO-DEWET (BIRD221997) funded under the BIRD 2022 program sponsored by the University of Padova.

Appendix A. Supplementary data

Supplementary data to this article can be found online at <https://doi.org/10.1016/j.nocx.2022.100143>.

References

- [1] Y. Hou, M. Yu, X. Chen, Z. Wang, S. Yao, Recurrent filmwise and dropwise condensation on a beetle mimetic surface, *ACS Nano* 9 (2015) 71–81.
- [2] A. Ghosh, S. Beaini, B.J. Zhang, R. Ganguly, C.M. Megaridis, Enhancing dropwise condensation through bioinspired wettability patterning, *Langmuir* 30 (2014) 13103–13115.
- [3] J. Huang, J. Zhang, L. Wang, Review of vapor condensation heat and mass transfer in the presence of non-condensable gas, *Appl. Therm. Eng.* 89 (2015) 469–484.
- [4] J.W. Rose, Dropwise condensation theory and experiment: a review, *Proc. Instit. Mech. Eng. Part A: J. Power Energy* 216 (2002) 115–128.
- [5] E. Colusso, et al., Solution-processed graphene oxide coatings for enhanced heat transfer during dropwise condensation of steam, *Nano Select* 2 (2021) 61–71.
- [6] S. Bortolin, M. Tancon, D. del Col, Heat transfer enhancement during dropwise condensation over wettability-controlled surfaces, *Surf. Wettability Eff. Phase Chang.* 29–67 (2022), https://doi.org/10.1007/978-3-030-82992-6_3.
- [7] J. Long, M. Zhong, H. Zhang, P. Fan, Superhydrophilicity to superhydrophobicity transition of picosecond laser microstructured aluminum in ambient air, *J. Colloid Interface Sci.* 441 (2015) 1–9.
- [8] L. De Ferri, P.P. Lottici, A. Lorenzi, A. Montenero, G. Vezzalini, Hybrid sol-gel based coatings for the protection of historical window glass, *J. Solgel. Sci. Technol.* 66 (2013) 253–263.
- [9] M. Tancon, et al., Dropwise condensation mechanisms when varying vapor velocity, *Appl. Therm. Eng.* 216 (2022), 119021.
- [10] T.L. Metroke, J.S. Gandhi, A. Apblett, Corrosion resistance properties of Ormosil coatings on 2024-T3 aluminum alloy, *Prog. Org. Coat.* 50 (2004) 231–246.
- [11] H. Jin, et al., Recent advances in emerging integrated antifouling and anticorrosion coatings, *Mater. Des.* 213 (2022), 110307.
- [12] R. Parin, et al., Heat transfer and droplet population during dropwise condensation on durable coatings, *Appl. Therm. Eng.* 179 (2020), 115718.
- [13] M. Mirafiori, R. Parin, S. Bortolin, D. Del Col, Experimental analysis of drop-size density distribution during dropwise condensation of steam, *J. Phys. Conf. Ser.* 1599 (2020).
- [14] Chemix - Draw Lab Diagrams, Simply. <https://chemix.org/>, 2022.
- [15] R. Parin, M. Sturaro, S. Bortolin, A. Martucci, D. del Col, Heat transfer during dropwise condensation of steam over a mirror polished sol-gel coated aluminum substrate, *Int. J. Therm. Sci.* 144 (2019) 93–106.
- [16] R. Parin, M. Rigon, S. Bortolin, A. Martucci, D. del Col, Optimization of hybrid sol-gel coating for dropwise condensation of pure steam, *Materials* 13 (2020) 878.
- [17] M. Basso, et al., Bioinspired silica-based sol-gel micropatterns on aluminum for humid air condensation, *J. Solgel. Sci. Technol.* 102 (2022) 466–477.
- [18] C.S. Sharma, C. Stamatopoulos, R. Suter, P.R. Von Rohr, D. Poulikakos, Rationally 3D-textured copper surfaces for Laplace pressure imbalance-induced enhancement in dropwise condensation, *ACS Appl. Mater. Interfaces* 10 (2018) 29127–29135.
- [19] D. Torresin, M.K. Tiwari, D. Del Col, D. Poulikakos, Flow condensation on copper-based nanotextured superhydrophobic surfaces, *Langmuir* 29 (2013) 840–848.
- [20] D. Del Col, R. Parin, A. Bisetto, S. Bortolin, A. Martucci, Film condensation of steam flowing on a hydrophobic surface, *Int. J. Heat Mass Transf.* 107 (2017) 307–318.
- [21] S. Kim, K.J. Kim, Dropwise condensation modeling suitable for superhydrophobic surfaces, *J. Heat Transf.* 133 (2011) 1–8.
- [22] P. Innocenzi, P. Falcaro, D. Grosso, F. Babonneau, Order-disorder transitions and evolution of silica structure in self-assembled mesostructured silica films studied through FTIR spectroscopy, *J. Phys. Chem. B* 107 (2003) 4711–4717.
- [23] R. Wen, S. Xu, X. Ma, Y.C. Lee, R. Yang, Three-dimensional Superhydrophobic nanowire networks for enhancing condensation heat transfer, *Joule* 2 (2018) 269–279.
- [24] D.J. Preston, D.L. Mafra, N. Miljkovic, J. Kong, E.N. Wang, Scalable graphene coatings for enhanced condensation heat transfer, *Nano Lett.* 15 (2015) 2902–2909.
- [25] A.T. Paxson, J.L. Yagüe, K.K. Gleason, K.K. Varanasi, Stable dropwise condensation for enhancing heat transfer via the initiated chemical vapor deposition (iCVD) of grafted polymer films, *Adv. Mater.* 26 (2014) 418–423.
- [26] M.H. Rausch, A.P. Fröba, A. Leipertz, Dropwise condensation heat transfer on ion implanted aluminum surfaces, *Int. J. Heat Mass Transf.* 51 (2008) 1061–1070.
- [27] M. Guglielmi, Sol-gel coatings on metals, *J. Sol-Gel Sci. Technol.* 8 (1997) 443–449.

- [28] J. Ma, et al., Condensation induced delamination of nanoscale hydrophobic films, *Adv. Funct. Mater.* 29 (2019), 1905222.
- [29] M.J. Juan-Díaz, et al., Study of the degradation of hybrid sol-gel coatings in aqueous medium, *Prog. Org. Coat.* 77 (2014) 1799–1806.
- [30] F.J.M. Ruiz-Cabello, et al., Testing the performance of superhydrophobic aluminum surfaces, *J. Colloid Interface Sci.* 508 (2017) 129–136.